

## Electronic Supplementary Material

### **Ag–Sn@MOFs heterostructure enables ultrasensitive voltammetric determination of vismodegib in serum and urine**

**Glowi Alasiri<sup>a</sup>, Ali M. Alaseem<sup>b</sup>, Razan Orfali<sup>b</sup>, Ramadan Ali<sup>c</sup>, Al-Montaser Bellah H. Ali<sup>d</sup>,**

**Mohamed M. El-Wekil<sup>d, e\*</sup>**

<sup>a</sup> Department of Biochemistry, College of Medicine, Imam Mohammad Ibn Saud Islamic University (IMSIU), Riyadh, 13317, Saudi Arabia.

<sup>b</sup> Department of pharmacology College of Medicine, Imam Mohammad Ibn Saud Islamic University (IMSIU), Riyadh 13317, Saudi Arabia

<sup>c</sup> Department of Pharmaceutical Chemistry, Faculty of Pharmacy, University of Tabuk, Tabuk 71491, Saudi Arabia

<sup>d</sup> Department of Pharmaceutical Analytical Chemistry, Faculty of Pharmacy, Assiut University, Assiut, 71526, Egypt

<sup>e</sup> Pharmaceutical Chemistry Department, Faculty of Pharmacy, Badr University in Assiut (BUA), 2014101, Assiut, Egypt

#### **Correspondence**

\* [mohamed.elwakeel@pharm.aun.edu.eg](mailto:mohamed.elwakeel@pharm.aun.edu.eg), [mohamed.mohamoud@ymail.com](mailto:mohamed.mohamoud@ymail.com)

## Instruments

The composite morphology was characterized by FE-SEM (JEOL JSM-6700F) and TEM (JEOL JEM-100CX II). Crystallinity and phase purity were confirmed by PXRD (Philips-FEI PW 1710) by matching diffraction patterns to JCPDS standards. Surface composition and chemical states were analyzed by XPS (PHI 5700 ESCA), including elemental content, metal oxidation states, and N/O functionalization. Electrochemical performance was assessed by CV and DPV using a VersaSTAT MC in a three-electrode cell with Ag-Sn@MOF/GCE as the working electrode, Pt wire as the counter, and Ag/AgCl (3 M KCl) as the reference, in phosphate buffer to evaluate charge-transfer kinetics, electrocatalysis, and VIS response. Dynamic light scattering (DLS) measurements were carried out using the ZEN 3600 Nano ZS instrument (Malvern, UK) to measure the surface charge. Specific surface area and pore size distribution were determined using BET analysis (TriStar II, Micromeritics). Functional groups were analyzed using Fourier transform infrared spectroscopy (FT-IR, Thermo Nicolet 670, Bruker, Germany).

## Electrochemical measurements

Electrochemical characteristics of the prepared electrodes were investigated using cyclic voltammetry (CV), electrochemical impedance spectroscopy (EIS), and differential pulse voltammetry (DPV). CV scans were collected over  $-0.2$  to  $0.6$  V at a scan rate of  $120$  mV s $^{-1}$  to compare redox responses and qualitatively probe electron-transfer kinetics at the electrode/electrolyte interface. EIS measurements were performed in the  $0.1$ – $10^6$  Hz frequency window at an applied potential of  $0.5$  V to evaluate interfacial charge transport; the charge-transfer resistance ( $R_{ct}$ ) was extracted from the impedance response as an indicator of electron-transfer efficiency. For analytical determination of VIS, DPV was conducted using the Ag–Sn@MOF/GCE under the optimized settings (potential window:  $-0.2$  to  $1.3$  V; pre-accumulation time:  $150$  s; modulation amplitude:  $0.076$  V; pulse width:  $0.054$  s; step potential:  $0.0035$  V), yielding a strengthened voltammetric signal and improved sensitivity for VIS quantification. Thermogravimetric analysis (TGA) was performed using a PerkinElmer TGA 4000 (USA), heating approximately  $1$  mg of sample from  $30$  to  $800$  °C at  $5$  °C min $^{-1}$  under nitrogen, allowing clear differentiation between framework decomposition and guest molecule release.

## **Preparation of real samples**

Following approval from the relevant ethics committee and after obtaining written informed consent, whole blood and urine samples were collected from healthy adult volunteers. Serum was separated by centrifugation (6000 rpm, 15 min), then deproteinized by adding 1 mL acetonitrile; the mixture was centrifuged again and the clarified supernatant was collected. The supernatant was concentrated using rotary evaporation, reconstituted in 0.1 M phosphate buffer (pH 7.0), and subsequently diluted 25-fold to minimize matrix interferences. Urine samples were analyzed directly without prior pretreatment. VIS was determined using the standard-addition approach with G-N@CDs as the fluorescent probe, and spike recoveries were calculated from the corresponding calibration curve. In compliance with Egyptian regulations, the study received ethical clearance from Assiut University and included only participants who had provided informed consent.

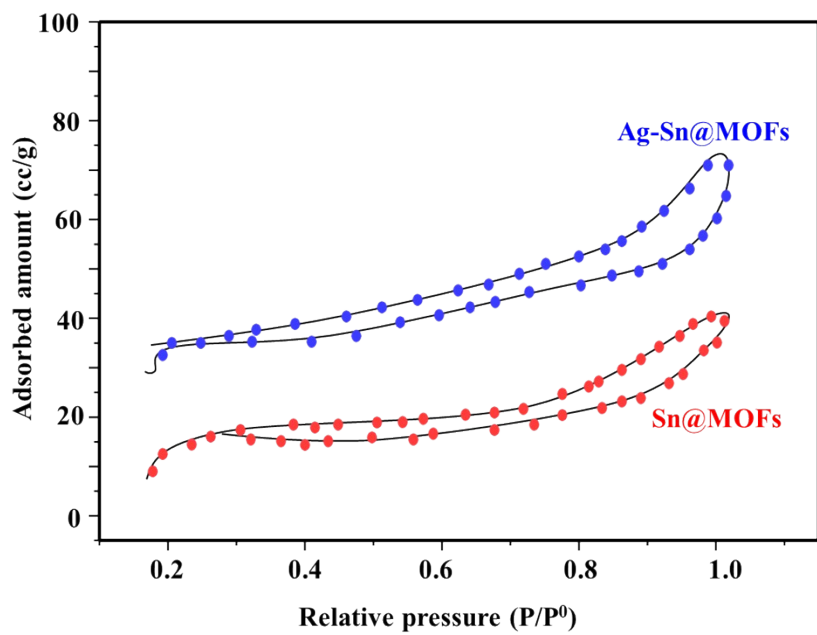


**Fig. S1** Nitrogen adsorption-desorption isotherm of Sn@MOFs and Ag-Sn@MOFs.

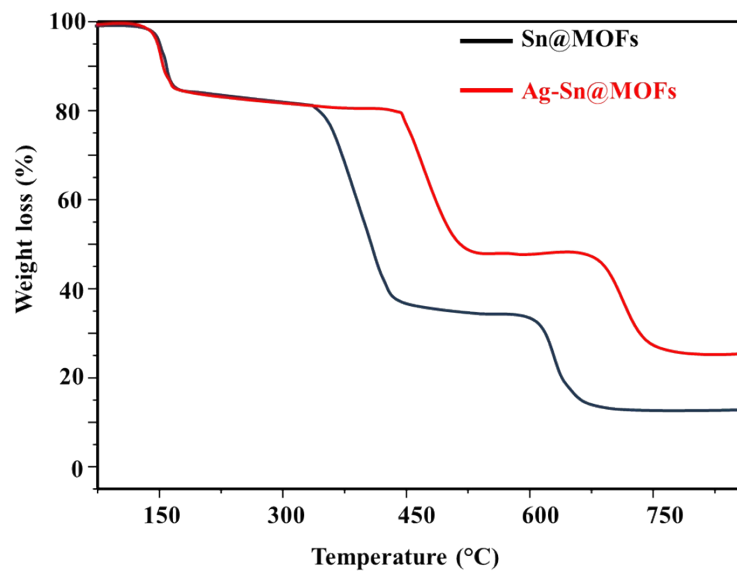


**Fig. S2** TGA of Sn@MOFs and Ag-Sn@MOFs.

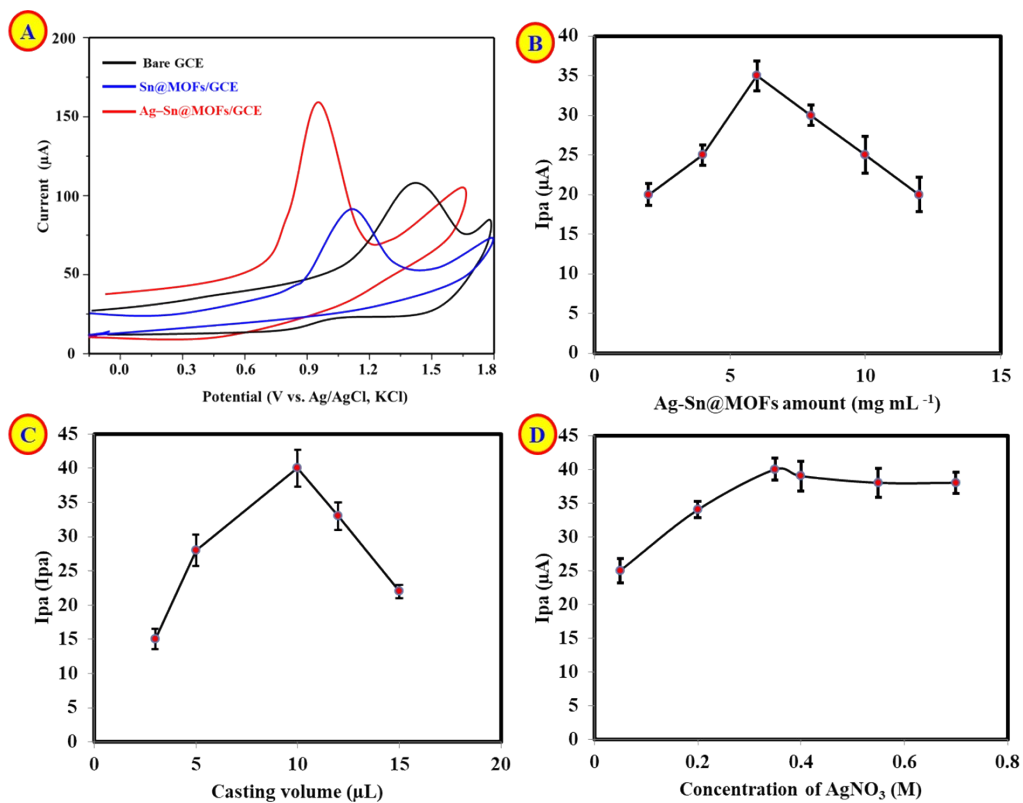


**Fig. S3** (A) CVs of 5.0  $\mu\text{M}$  VIS at bare GCE, Sn@MOFs/GCE, and Ag-Sn@MOFs/GCE; (A) influence of Ag-Sn@MOFs' concentration on the electrocatalytic oxidation of 50 nM VIS using DPV; (C) Effect of casting volume of Ag-Sn@MOFs/GCE on the electrocatalytic oxidation of 50 nM VIS using DPV; (D) Influence of  $\text{AgNO}_3$  concentration on the the electrocatalytic oxidation of 50 nM VIS using DPV.

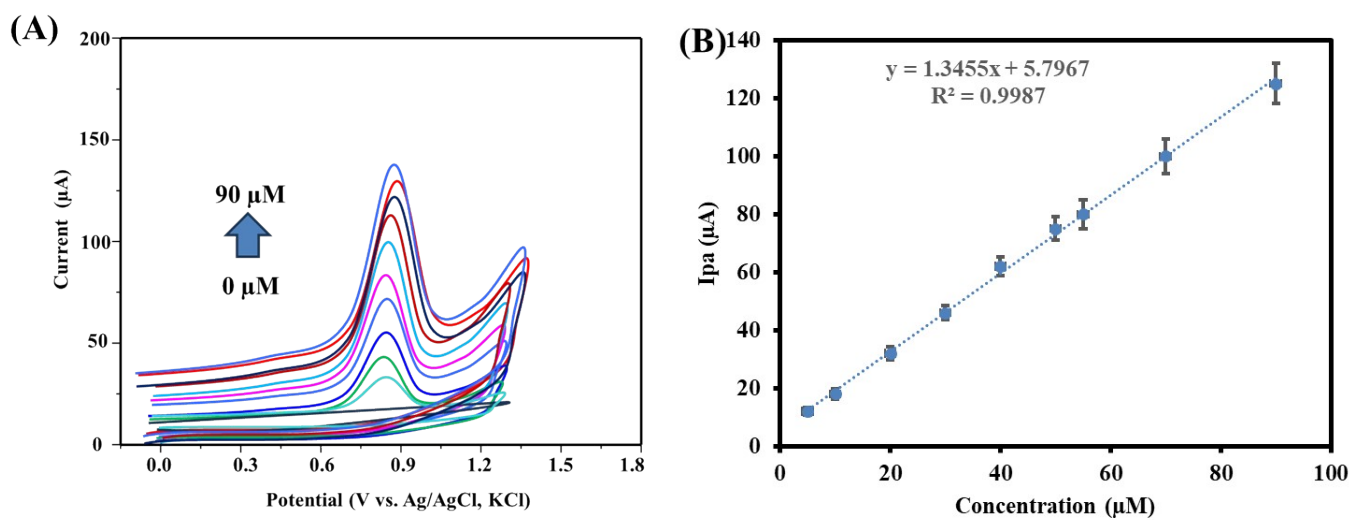


**Fig. S4** (A) CV of different concentrations of VIS (0-90 μM) at Ag-Sn@MOFs/GCE. (B) Calibration plot of I<sub>pa</sub> vs. concentration of VIS. Number of replicates are five.

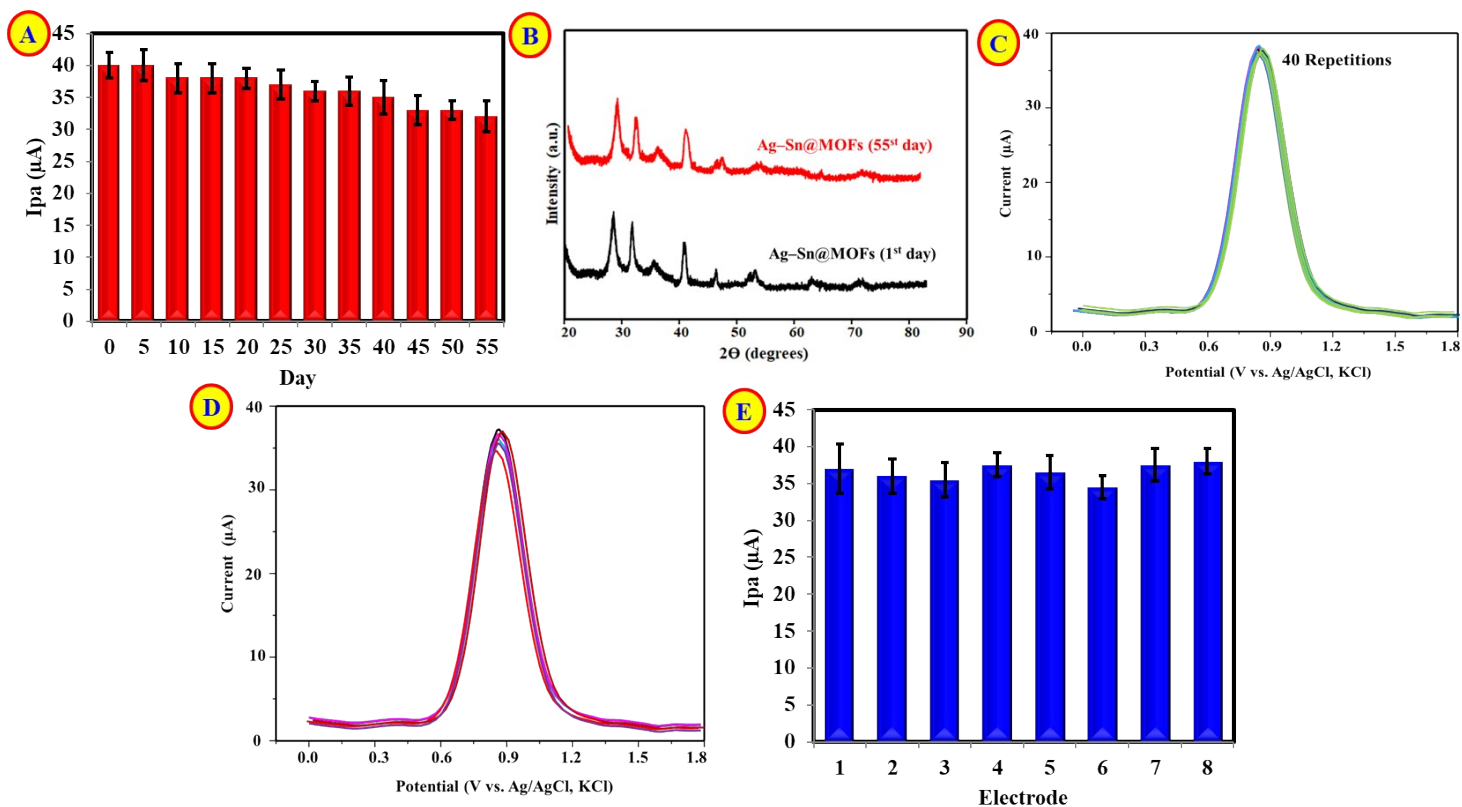


**Fig. S5** Performance validation of the Ag-Sn@MOFs/GCE for 50 nM VIS in phosphate buffer (pH 7.0): (A) storage stability, (B) XRD pattern at 1<sup>st</sup> and 55<sup>th</sup> day(s), (C) 40-scan repeatability, and (D, E) inter-electrode reproducibility. Error bars show SD (n = 3).